ISBN: 978-3-95450-227-1 ISSN: 2673-5490 doi:10.18429/JACoW-IPAC2022-TUPOMS062

OVERALL PERFORMANCE OF 26 POWER STATIONS AT 400 kW - 352 MHz

C. Pasotti*, A. Cuttin, Elettra Sincrotrone Trieste S.C.p.A., Trieste, Italy

Abstract

The spoke cavities section of the European Spallation Source (ESS) linac will be powered by 26 Radio Frequency Power Stations (RFPSs). Each RFPS delivers 400 kW of Radio Frequency (RF) power at 352.21 MHz in pulsed mode at a repetition rate up to 14 Hz and a 5 % duty cycle, thanks to a twin tetrodes RF power sources integration. This equipment belongs to the Italian In-Kind Contributions (IKCs) to ESS. Elettra Sincrotrone Trieste S.C.p.A (Elettra) is responsible for the development, manufacturing and commissioning of the RFPSs and is managing the RFPS manufacturing contract awarded to European Science Solutions s.r.l (ESS-It). So far, 24 units have been delivered and, by mid 2022, the entire contribution, plus a complete spare unit, will be delivered to ESS. The overall performance of the RFPSs, the lessons learned, and the optimizations adopted along the manufacturing process and the difficulties that the COVID-19 pandemic has posed along the way are presented in this contribution.

INTRODUCTION

The European Spallation Source (ESS) project has the objective of generating neutrons by spallation reaction of protons on a tungsten rotating target at an average beam power of 5 MW. It is carried out by more than 20 European partner laboratories, and hosted by Sweden and Denmark [1]. As a founding member of ESS European Research Infrastructure Consortium, Italy participates to the project as an In-Kind (IK) partner.

Within this framework, the Radio Frequency Power Stations (RFPSs), provided by European Science Solutions s.r.l (ESS-It) with the supervision of Elettra Sincrotrone Trieste S.C.p.A (Elettra), represent one of the Italian In-Kind Contributions (IKCs) to ESS [2]. They will power 26 spoke cavities, installed in the first segment of the superconducting section of the proton linac.

After nearly two years of manufacturing and testing, mainly carried out during the COVID-19 pandemic with an innovative approach [3], the main results of 26 Factory Acceptance Tests (FATs), out of 27, are presented, providing new insights about this IKC. As of the date of writing, 24 RFPS units have already been delivered to ESS, with only the last batch to be shipped.

The manuscript is organized as follows: the next section offers an overview of the RFPS and its sub-systems; then, the FAT protocol is detailed in its main steps. After that, the RFPS performance is presented in terms of Radio Frequency (RF) key parameters, resulting from FAT measurements; finally the results are discussed and next steps proposed.

* cristina.pasotti@elettra.eu

Figure 1: FAT setup. The six-racks RFPS is shown with the middle covers removed, revealing the twin cavities configuration. On the far left, the rack of the required instruments.

RFPS OVERVIEW

With a very compact design, the RFPS achieves 400 kW of peak power at 352.21 MHz, with a pulse length up to 3.5 ms and a repetition rate up to 14 Hz [4].

It consists of two identical branches, each one having a Solid State Driver (SSD) (KDP10000) followed by a tetrode-cavity Power Amplifier (PA) (Thales TH595A and TH18595A). The two branches are fed by a single RF distribution module, which provides amplitude adjustment on one arm, and phase adjustment on the other. The signals are then added together by means of a 3 dB hybrid combiner.

The RFPS features an original Supervisory Control System (SCS) that combines standard Programmable Logic Controller (PLC) equipment with specifically designed Field Programmable Gate Array (FPGA) boards for handling the interlocks in a fast way (in the order of 1×10^{-6} s with respect to 1×10^{-3} s specified for the tetrode).

In Fig. 1, a RFPS can be seen in the typical FAT setup. From left to right, the first rack holds the SSDs, the RF distribution module, the Human Machine Interface (HMI) and the main PLC module of the SCS. The second rack is dedicated to 4 screen and control grid Power Supplies (PSs), and Alternate Current (AC) distribution. In the middle, the twin TH18595A cavities are placed, together with their ancillary equipment. The fifth and sixth rack contain the High Voltage (HV) PS, supplying the anodic voltage to both tetrodes. It features a switching power converter, a capacitor bank, a solid state series switch. and a FPGA module of the SCS.

FAT OVERVIEW

The FAT process is conceived in a way that allows to individually test the RFPS sub-systems, and, at the same time, to avoid useless downtime between subsequent steps. The test sequence is such that the machine is progressively put into

ISBN: 978-3-95450-227-1 ISSN: 2673-5490 doi:10.18429/JACoW-IPAC2022-TUPOMS062

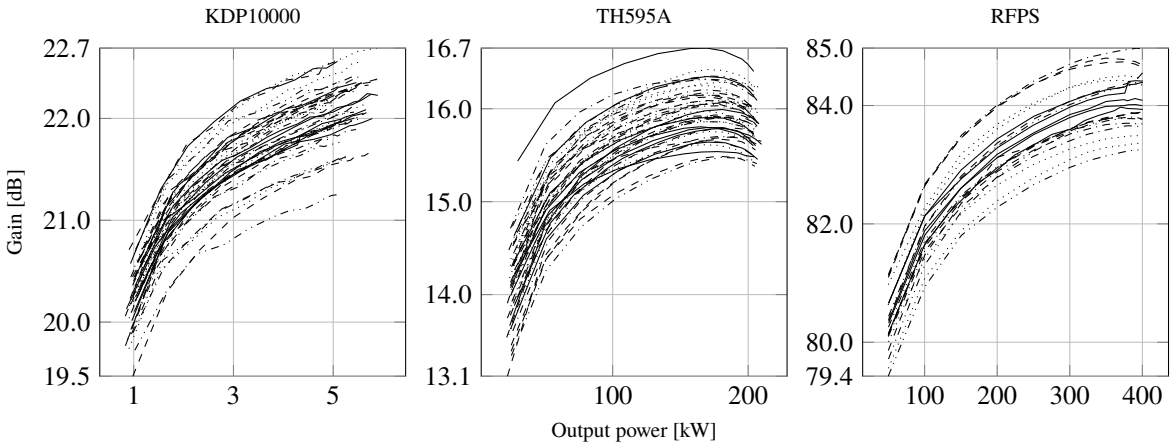

Figure 2: Evaluation of gain at different stages of the amplification chain.

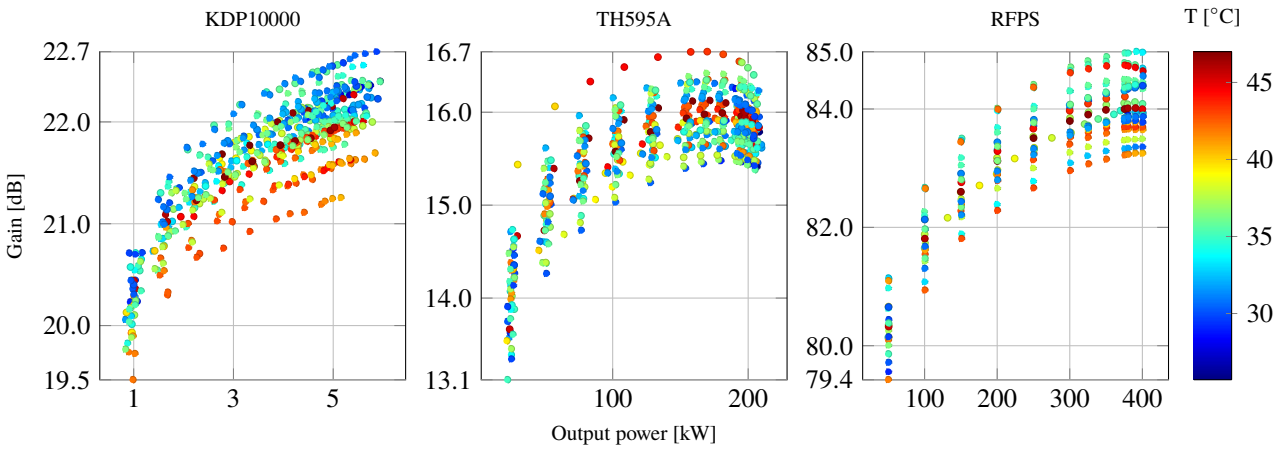

Figure 3: Visualization of the effect on the gain of the temperature change of the coolant.

operation, from the simple turn-on of the AC main breaker, up to the generation of the full RF power, thus optimizing the time required to carry out the entire procedure.

The optimal sequence of checks foreseen by the FAT protocol is as follows:

1. Interlocks managed by the FPGA-based boards.
2. Interlocks managed by the PLC SCS.
3. Direct Current (DC) and RF signals calibration.
4. Hard Remote Control Port (HRCP).
5. Tuning of TH595A tetrodes and RF output power P_{out} optimization.
6. RFPS gain and RF efficiency.
7. Electrical grid consumption and flicker compensation.
8. Pulse parameters and HMI data.
9. Pulse repetition rate and RF driving signal.
10. Intra-Pulse and Pulse-to-Pulse output signal quality.
11. Duration test: RFPS working at 400 kW for 24 h.

RFPS PERFORMANCE

With respect to the FAT protocol previously detailed, this section presents the main results. Many of the verifications (including, but not limited to, items 1, 2 and 4) essentially have a Pass/Fail outcome. In case of a Fail, the majority (if not all) of the times, the main reason was the infant mortality of some sub-assembly, due to manufacturing defects. Also, such tests ensure that the RFPS can be safely operated, and that it is able to protect itself and the operator.

With this in mind, it is of interest to look at the results that provide a characterization of the RFPSs from an RF point of view. The evaluation of the gain at the output (G_{RFPS}), and at intermediate amplification stages (G_{SSD}, G_{TH595A}) of each RFPS is as follows.

Gain Evaluation

After the calibration step of item 3, digital readings presented by the HMI are considered trustworthy, within the accuracy of said calibration, and therefore P_{out} measurements can be obtained directly by recording the the HMI display.

For every RFPS, the input P_{in} and output P_{out} power levels were recorded at predefined intervals, so as to have consistent data sets. The readings from the HMI included also measurement of voltages, currents, and temperatures of the considered stages. Readings were taken from 50 kW to 300 kW at 50 kW increments, and also at 325, 350, 375, 380, 390, 400 kW, thus having care to refine the power level increment towards the end of the linear region.

ISBN: 978-3-95450-227-1 ISSN: 2673-5490 doi:10.18429/JACoW-IPAC2022-TUPOMS062

At this point, the gain of the RFPS and of its intermediate amplification stages can be evaluated. In Fig. 2, gain of KDP10000 SSD (G_{SSD}), the TH595A tetrode (G_{TH595A}), and of the overall RFPS (G_{RFPS}), is shown, respectively, for each unit. While the RFPS plot presents 26 traces, KDP10000 and TH595A plots show twice the traces, because of the twin configuration. Each plot displays the minimum and the maximum values resulting from the measurement.

Temperature Correlation

Readings from the HMI also include the temperature of the cooling water, therefore allowing to correlate the gain variations with it. By adding this information, one obtains Fig. 3, where the colour of each data point corresponds to the temperature of the coolant at the inlet.

This evaluation is of interest because of the nature of the cooling system available at the test facility of ESS-It. Indeed, it features an open-air heat exchanger; therefore the cooling water can only be as cool as the surrounding ambient temperature. Such limitation affected the measurements, that were therefore subject to seasonal variations.

To further prove the impact of this constraint, Fig. 4 shows the inverse correlation between the gain and the temperature variation during the 24 h duration test of item 11. For each data group, the lower the temperature, the higher the gain.

This is also the reason why the gain G is shown with respect to P_{out}, and not as usual with respect to P_{in}. While the latter approach allows to better see the linear region of an amplifier, the visualization of Figs. 2 and 3 is the only one that allows to compare the performance of each unit with respect to the others in a meaningful way.

DISCUSSION

By comparing results of Fig. 2 with technical specifications [5], it is possible to state that the RFPS as a unit, and individually the tetrode and SSD, meet their requirements with margin to spare.

Specifically, all the RFPSs achieve the required gain ($G_{RFPS} \geqslant 76$ dB) already at the lowest output power level considered. Indeed, the smallest gain value recorded is 79.4 dB at $P_{out} = 50$ kW, well outside the optimal working region. At nominal power, the margin exceeds 6 dB. The gain requirement is also met by the PAs ($G_{TH595A} \geqslant 15$ dB), with less margin. The behaviour of SSDs is in agreement with the specification (with a margin ranging from 0.5 dB to 2 dB), even if it has been affected by the seasonal change in temperature of the coolant, as clearly visible in Fig. 3.

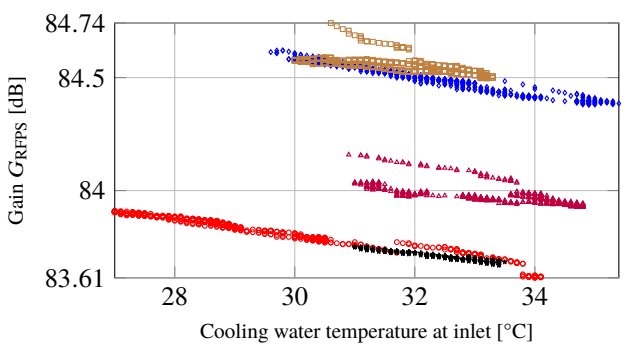

Figure 4: Gain changes due to coolant temperature variation. Each mark style correspond to a different RFPS.

Figure 3 makes additional considerations possible. Given that G_{SSD} improves with better cooling, a stable temperature of the coolant should provide a better grouping of the KDP10000 characteristics, with less dispersion. TH595A tetrodes, instead, show less correlation with the temperature. Therefore, the primary function of their coolant is to take away the power dissipated at the anode, irrespective to its absolute temperature. As a result, G_{RFPS} is not as affected by the temperature as G_{SSD} is.

So, the choice of cooling the RFPS using two different circuits (medium temperature for SSDs and high temperature for PAs) is consistent with the measured data.

CONCLUSION

The IKC of 26 RFPSs (plus one spare), supervised by Elettra, is almost completed, with 26/27 units tested and 24/27 units delivered. Measured data behave in accordance with the test conditions and technical expectations. RF performance indicators are satisfactory with margin. Further data analysis will provide a comprehensive characterization of the RFPS system.

ACKNOWLEDGEMENTS

The authors express their appreciation and gratitude to the personnel of ESS-It involved in the FAT process.

REFERENCES

[1] R. Garoby, *et al.* “The European Spallation Source Design”, *Physica Scripta*, vol. 93, no. 1, p. 014001, December 2017. doi:10.1088/1402-4896/aa9bff

[2] S. Gammino, A. Fabris, and M. Lindroos, “The Italian contribution to the construction of the linac for the European spallation source”, *Riv. Nuovo Cim.*, vol. 44, no. 7, pp. 365–396, Jul. 2021. doi:10.1007/s40766-021-00021-y

[3] C. Pasotti, A. Cuttin, A. Fabris, A. Frizzi, M. Rossi, and G. Zardi, “Remote Commissioning of 400 kW 352 MHz Amplifiers”, in *Proc. IPAC’21*, Campinas, Brazil, May 2021, pp. 2332–2334. doi:10.18429/JACoW-IPAC2021-TUPAB353

[4] C. Pasotti, M. Cautero, T. N. Gucin, C. A. Martins, and R.A. Yogi, “Radio Frequency Power Stations for ESS LINAC Spoke Section”, in *Proc. IPAC’19*, Melbourne, Australia, May 2019, pp. 4346–4348. doi:10.18429/JACoW-IPAC2019-THPTS102

[5] C. Pasotti, “Fornitura di n. 26 stazioni di potenza a radiofrequenza da 400 kW – 352 MHz, per il progetto ESS (European Spallation Source)”, https://servizi-dac.dsi.infn.it/index.php/gestioneavvisi/dettaglioAvviso/2062720/0/2